

1

2 **Vessel wall reinforcement metrics as drought resistance indicators in angiosperm**

3 **fossil wood assemblages**

4

5

6 Hugo I. Martínez-Cabrera^{1*}, Emilio Estrada-Ruiz², and Carlos Castañeda-Posadas³

7

8

9 ¹Museo Paleontológico de Múzquiz, Adolfo E. Romo 1701, La Cascada, 26343, Santa
10 Rosa de Múzquiz, Melchor Múzquiz, Coahuila, México.

11 ²Departamento de Zoología, Escuela Nacional de Ciencias Biológicas – Instituto
12 Politécnico Nacional, Prolongación de Carpio y Plan de Ayala s/n, 11340, Ciudad de
13 México, México.

14 ³Benemérita Universidad Autónoma de Puebla, Facultad de Ciencias Biológicas,
15 Laboratorio de Paleontología, Blvd. Valsequillo y Av. San Claudio, BIO 1, Ciudad
16 Universitaria, Col. Jardines de San Manuel, Puebla, 72570, Mexico.

17

18 ***Author for correspondence:** hugomartinez2w@gmail.com

19

20

21

22

23

24

25 .

26 **Abstract**

27 **Background:** Plant ecologists have developed methods to measure xylem drought
28 resistance but these cannot be used in fossil woods. There is, however, one anatomical
29 trait highly correlated with cavitation resistance: the squared vessel-wall thickness-to-
30 span ratio $((t/b)_h^2)$. This metric though, could be in many cases impractical to measure
31 in fossil samples because they often are small and sample sizes are seldom reached.

32 **Questions:** are there alternative anatomical metrics that could be used instead of $(t/b)_h^2$
33 to infer drought resistance of fossil wood assemblages?

34 **Study site and dates:** 279 species belonging to 14 extant communities from North and
35 South America. Three fossil wood floras from the Oligocene and Miocene of Mexico.

36 **Methods:** We calculated three alternative wall reinforcement metrics to determine their
37 relationship with $(t/b)_h^2$ and drought resistance. These are based on vessel diameter and
38 vessel wall thickness.

39 **Results:** We found that one of the alternative metrics $((t/b)_{\text{hydraulic mean}}^2)$ could
40 potentially be used instead of $(t/b)_h^2$. The widely measured vessel wall-to-lumen ratio
41 (VWLR), was the closest related to climate, and thus helpful in identifying broad
42 precipitation differences among floras. VWLR and $(t/b)_h^2$ might be describing slightly
43 different ecological axes of ecological variation, with the latter associated with
44 investment in support tissue, in addition to water availability alone.

45 **Conclusions:** Some of the alternative metrics we explored can be used, in combination
46 with other functional traits, to better describe fossil forest functional strategies.

47 **Key words:** drought resistance; fossil woods; paleoecology; vessel wall reinforcement;
48 wood anatomy.

49

50

51 **Introduction**

52 Because the diffusion coefficient of water is larger than for CO₂ (Lambers *et al.*, 1998),
53 carbon fixation could be an expensive process in terms of water expenditure. Per each
54 mole of CO₂ fixed during photosynthesis, over 100 moles of water are transpired
55 (Cramer *et al.* 2008). Efficient carbon fixation therefore requires an equally efficient
56 hydraulic system to meet the water requirements of the evaporative surface during the
57 photosynthesis. For this reason, stem hydraulic capacity is directly related to growth
58 rate (e.g. Machado & Tyree 1994) and photosynthetic capacity (Santiago *et al.* 2004).
59 There is a general relationship between vessel diameter (the main determinant of xylem
60 hydraulic efficiency, Poorter 2008, Zanne *et al.* 2010) and environmental conditions
61 such that, across vegetation types (in low latitudes and altitudes), water availability and
62 vessel size are positively related (Carlquist 1988, Wheeler *et al.* 2007). In wet warm
63 environments, plants maximize hydraulic efficiency by decreasing water flow resistance
64 in the xylem (i.e. by having larger vessel diameter) to maintain high transpiration rates,
65 carbon fixation and growth (Tyree 2003). On the other hand, in dry environments these
66 large, efficient vessels are at disadvantage since they are more likely to experience
67 drought induced cavitation (because the likelihood of finding large pores in the pit
68 membrane increases with vessel size; Wheeler *et al.* 2005) and/or their walls are more
69 likely to experience mechanical failure (Hacke & Sperry 2001, Hacke *et al.* 2001,
70 Jacobsen *et al.* 2005).

71 Plants from drier regions are generally more able to cope with drought because
72 cavitation in small vessels occurs at lower water potential than in wet adapted plants
73 with larger vessel diameters (Sperry & Pockman 1993, Kolb & Sperry 1999). The
74 ecological outcome of vessel cavitation is the disruption of the water column, which
75 results in the reduction of plant water supply to leaves (Meinzer *et al.* 2001), and a

76 consequential decrease in stomatal conductance (Pratt *et al.* 2005) and photosynthesis
77 (Brodribb & Feild 2000). Knowing how these wood anatomical traits related to drought
78 resistance vary in modern ecosystems, can help us to infer some aspects of fossil forest
79 function, particularly of those traits associated with adaptations to water deficit.

80 In living plants, cavitation resistance is measured using the water potential at
81 which there is a determined percent loss of hydraulic conductivity. This percent is
82 usually 50% (P_{50}). As P_{50} cannot be directly measured in fossil woods, the squared
83 vessel-wall thickness-to-span ratio ($(t/b)_h^2$) which is tightly related with P_{50} (Hacke *et*
84 *al.* 2001), has been used to infer its values in a fossil wood assemblage (Martínez-
85 Cabrera & Estrada-Ruiz 2014). $(t/b)_h^2$ is a good indicator of resistance to water stress
86 because it explains up to 95% of the variation in P_{50} (Jacobsen *et al.* 2005). $(t/b)_h^2$ is,
87 however, hard to measure because it only considers those vessel pairs that fall within 3
88 to 5 μm of the hydraulic diameter. Because the small size of many fossil woods, it is
89 common to find very small sample sizes with no more than a couple of vessel pairs
90 falling within 5 μm of the mean hydraulic diameter. Besides, many fossil assemblages
91 have species with exclusively solitary vessels, rendering this metric impractical. Given
92 the promising results of the vessel wall reinforcement in providing ecological
93 information in wood paleofloras (Martínez-Cabrera & Estrada-Ruiz 2014), here we
94 explored if more easy-to-measure metrics are equally informative. Specifically, 1) we
95 used anatomical data from extant communities to quantify how much of the variation of
96 the squared vessel-wall thickness-to-span ratio is explained by three alternative metrics,
97 and if one of these could be used to infer drought resistance. In addition, 2) we
98 correlated these alternative vessel wall reinforcement metrics with climate variables to
99 if they are likely to provide information about the growing conditions and functional
100 characteristics of fossil floras. Finally, 3) we calculated the metric with tighter relation

101 with climate variables (vessel wall-to-lumen ratio) of three relatively well known fossil
102 wood assemblages, to contrast with the functional and climate interpretations provided
103 by other studies in those sites.

104

105 **Material and methods**

106 We analyzed two different databases (Table S1). With the first database, that includes 62
107 species from a variety of environments in North and South America (Martínez-Cabrera
108 *et al.* 2009), we tested if $(t/b)_h^2$ variation is mirrored by more simple versions of it, such
109 as $(t/b)_{\text{mean}}^2$, $(t/b)_{\text{hydraulic mean}}^2$, and VWLRT. The squared vessel-wall thickness-to-span
110 ratio $(t/b)_h^2$ (where t , is the thickness of the double-wall between two adjacent vessels
111 and b is the diameter of the conduit closest to the hydraulic mean diameter), is
112 exclusively measured in vessel pairs within 3 to 5 μm of the hydraulic diameter. The
113 mean hydraulic diameter has to be determined before locating the target vessel pairs. In
114 the alternative metrics we explored here ($(t/b)_{\text{mean}}^2$ and $(t/b)_{\text{hydraulic mean}}^2$), t is the mean of
115 vessel wall thickness times two, while b is simply the mean vessel diameter and the
116 mean hydraulic diameter of the sample, respectively. The difference between $(t/b)_h^2$ and
117 $(t/b)_{\text{hydraulic mean}}^2$ is that in the former, t only includes the vessel pairs falling within 5 μm
118 of the mean hydraulic diameter, while in the latter, t is simply the mean hydraulic
119 diameter of the sample. In this database, vessel lumen diameter, including mean vessel
120 diameter and hydraulic mean was calculated using diameters of circles with the same
121 area as the individual vessel lumens. The hydraulic mean was calculated as the sum of
122 the contribution of all conduit diameters ($\sum d^5$) divided by the total number of vessels
123 ($\sum d^4$) (see Martínez-Cabrera & Estrada-Ruiz 2014 for details). VWLR is the ratio
124 between wall thickness and the mean vessel diameter. We calculated the P_{50} values
125 (based on the general formula $P_{50} = 20.662 - 154.646x$, where x was $(t/b)_h^2$, $(t/b)_{\text{mean}}^2$ or

126 $(t/b)_{\text{hydraulic mean}}^2$) for each one of the three metrics and compared the estimates to assess
127 the suitability of $(t/b)_{\text{mean}}^2$ and $(t/b)_{\text{hydraulic mean}}^2$, as an alternative to the P_{50} values
128 predicted by $(t/b)_h^2$. The original formula was derived using $(t/b)_h^2$ (formula provided by
129 Uwe Hacke).

130 For our second analysis, we then combined the climate (MAP, MAT, and PET)
131 and VWLR data from the database mentioned above (Martínez Cabrera *et al.* 2009)
132 with the second database (Martínez-Cabrera & Cevallos-Ferriz 2008). This database
133 comprises extant floras growing under a wide range of environments and was used to
134 determine the extent to which VWLR is environmentally driven. As $(t/b)_h^2$ was not
135 measured in that study (Martínez-Cabrera & Cevallos-Ferriz 2008), it was not analyzed
136 here. Lastly, we analyzed the extant communities' VWLR with that of three fossil
137 localities, El Cien Formation (Oligocene-Miocene; Martínez -Cabrera & Cevallos-
138 Ferriz 2008), Las Guacamayas (Miocene, Chiapas, Mexico) and La Mina (Miocene,
139 Tlaxcala, Mexico) (Castañeda-Posadas 2007) to establish the scope and resolution of
140 the paleoecological information that this anatomical trait provides. We did not have the
141 mean hydraulic diameter for the fossil woods, and therefore it was not possible to
142 estimate P_{50} values based on $(t/b)_{\text{hydraulic mean}}^2$, and decided not to use the mean vessel
143 diameter because, as we discuss below, the P_{50} calculated with $(t/b)_{\text{mean}}^2$ has larger
144 associated errors.

145

146 **Results and Discussion**

147 *Relationship between the squared vessel-wall thickness-to-span ratio and alternative*
148 *metrics.* As expected, $(t/b)_h^2$ was more tightly related with $(t/b)_{\text{hydraulic mean}}^2$ ($R^2 = 0.83$, P
149 < 0.001), than to $(t/b)_{\text{mean}}^2$ ($R^2 = 0.54$, $P < 0.001$) or VWLR ($R^2 = 0.54$, $P < 0.001$)
150 (Figure 1). Consequently, the P_{50} values based on $(t/b)_h^2$ are more similar to those

151 calculated using $(t/b)_{\text{hydraulic mean}}^2$, ($R^2 = 0.83$, $P < 0.001$; Figure 2A) than those based on
152 $(t/b)_{\text{mean}}^2$ ($R^2 = 0.54$, $P < 0.001$). $(t/b)_{\text{mean}}^2$ tends to overestimate P_{50} values (cavitation at
153 more negative water potentials), especially in drier communities (Figure 2B), but this is
154 not the case for $(t/b)_{\text{hydraulic mean}}^2$. Our results suggest that if $(t/b)_h^2$ is not possible to
155 measure in a particular fossil wood assemblage, $(t/b)_{\text{hydraulic mean}}^2$ could be used to
156 broadly infer cavitation resistance. We suggest, however, that comparing P_{50} estimates
157 of fossil wood assemblages calculated with different metrics (*i.e.* P_{50} vs. $P_{50 \text{ hydraulic}}$)
158 should be avoided as the estimated error varies (Figure 2).

159

160 *Relationship between wall reinforcement metrics climate.* In general, vessel
161 reinforcement (all four metrics) increases with temperature (MAT) and potential
162 evapotranspiration (PET) and decreases with precipitation (MAP). MAP was the
163 climate variable that better explained variation of all four-vessel reinforcement metrics
164 (Figure 3A), but its relationship with VWLR was the tightest. VWLR was the
165 anatomical trait more closely related to all climate variables (Figure 3, Table 1). In this
166 sense, $(t/b)_h^2$ and VWLR seem to be describing a slightly different ecological axis of
167 variation. Based on our results, VWLR has more potential as a tool in paleoclimate
168 prediction, while $(t/b)_h^2$ is describing, in addition to climate, cavitation resistance and
169 investment in support, and can thus offer a supplementary layer of paleoecological
170 information. Although fiber characteristics are the main determinants of investment in
171 support (*i.e.*, wood density, Hacke *et al.* 2001), the link between wood density and
172 $(t/b)_h^2$ is via a coordinated variation between fiber and vessel wall-to-lumen ratios
173 (Hacke *et al.* 2001). Jacobsen *et al.* (2005) proposed that the link between wood density
174 and $(t/b)_h^2$ is through the indirect effect of fibers reinforcing vessel walls, since higher
175 $(t/b)_h^2$, in their study, was not associated with a decrease conduction efficiency.

176 However, $(t/b)_h^2$ is not always correlated with the proportion of fibers surrounding
177 vessels (*i.e.*, species with extremely dense wood might have vasicentric parenchyma;
178 Martínez-Cabrera *et al.* 2009). Although, vessel implosion resistance has been rarely
179 observed (Bass 1986), Hacke *et al.* (2001) argue that incipient wall break can provoke
180 cavitation and stop vessel implosion. Regardless the mechanism linking both variables
181 might be, the relationship of $(t/b)_h^2$ with xylem density is clearly useful since it can shed
182 light on the ecological strategies of fossil assemblages (*e.g.*, investment in support, or
183 life history traits such as growth rates, survival, and life span, Muller-Landau 2004),
184 besides the more obvious link to resistance to drought.

185 In the combined dataset, variation in VWLR was again better explained by MAP
186 (Table 1, Figure 4). Since the dataset had 15 outliers, was not normally distributed
187 (Shapiro-Wilk test = 0.91, $P < 0.001$, by group Shapiro-Wilk test 5 out of 14
188 communities had not normal distribution, Table S2), and the variance was not
189 homogeneous among groups (Levene test = 3.8, $P < 0.001$), we performed a Welch one-
190 way test (instead of a one-way ANOVA) to determine if there significant differences in
191 VWLR between communities. We found significant overall differences among
192 communities (Welch = 20.6, $P < 0.001$, $N = 279$), as well as differences between
193 community pairs (Games-Howell test is presented in Table S3). Drier communities had
194 vessels with thicker walls relative to their diameter (Figure 5A). These differences are
195 in general recognized by the Games-Howell test, especially when communities on
196 opposite sides of the MAP gradient are compared (Table S3). Despite its clear
197 relationship with the environment, the resolution of VWLR allows to distinguish only
198 broad MAP differences, these differences are harder to detect among communities
199 growing at similar MAP values (*i.e.*, communities growing under a MAP below 663
200 mm, not significantly different among them).

201

202 *Analysis of wall-to-lumen ratio trends in three Mexican fossil wood assemblages.* All
203 three fossil assemblages were significantly different from the drier sites (< 663 mm).
204 From the analysis of a subset of communities only including the tropical wet/semi
205 deciduous sites (Figure 5B; Games-Howell test Table S4) and the fossil wood localities,
206 we found that the VWLR of Las Guacamayas (Miocene,) and El Cien Formation floras
207 (Oligocene-Miocene) had vessels with significantly lower values of reinforcement than
208 the semi-deciduous forest from Chamela (798 mm) and had significantly higher
209 reinforcement values than the super humid tropical rain forest of Los Tuxtlas (4556
210 mm). While La Mina (Miocene, Tlaxcala) locality, was only different from the semi-
211 deciduous forest. These results generally agree with previous paleoecological and
212 paleoclimate analyses of those localities. Paleoclimate models suggest that La Mina and
213 Las Guacamayas floras grew under high humidity (MAP= 2172 and 1866 mm
214 respectively) and temperature (MAT > 25 °C), and an indistinct or short dry season,
215 conditions typically present in tropical rain forest (Castañeda-Posadas, 2007). The case
216 of La Mina is interesting since it has high prevalence of tropical genera such as
217 *Terminalia*, *Cedrela* and cf. *Pterocarpus*, and together with its predicted MAP and low
218 VWLR, not statistically different to the wettest extant tropical rain forest we analyzed,
219 suggest low drought resistance. It is however, worth noting that the estimated wood
220 density for this community is high (Martinez-Cabrera *et al.* 2012), which might be
221 indicating a higher drought resistance than VWLR alone might suggest. It has been
222 found that trees with denser wood are capable to retain more water and survive lower
223 water potential (trees with high wood density have lower leaf turgor loss point, Fu &
224 Meinzer 2019). This merits further research of the anatomy of this locality to evaluate
225 if the thicker fibers (hence the high predicted wood density), might be buttressing

226 vessels as has been hypothesized (Jacobsen *et al.* 2005), as La mina flora woods have
227 relatively thin walls relative to their lumen (low VWLR).

228 El Cien Formation flora is functionally and compositionally similar to the semi-
229 deciduous forests of the western coast of Mexico (*i.e.* Chamela). Here we found
230 significantly lower VWLR values of El Cien Formation woods, suggesting that
231 cavitation occurred at less negative water potential than in its living homologous
232 Chamela. El Cien Formation flora has a strikingly similar estimated wood density to
233 Chamela (Martínez-Cabrera *et al.* 2012), but dissimilarities in conduction efficiency and
234 now in vessel wall reinforcement, highlight the value of incorporating more functional
235 metrics in paleoecological analyses to recognize these nuances in fossil forest function,
236 as was also the case for La Mina locality.

237 The use of the vessel wall reinforcement metric calculated with the mean
238 hydraulic diameter ($(t/b)_{\text{hydraulic mean}}^2$) can be used as a sound approximation of the
239 original $(t/b)_h^2$, if this is impractical to measure. We found that the cavitation resistance
240 (P_{50} values) estimated with $(t/b)_{\text{hydraulic mean}}^2$ is close to those obtained with $(t/b)_h^2$. As the
241 metrics have different degrees of uncertainty, we suggest avoid comparing floras using
242 P_{50} estimates calculated with different wall reinforcement metrics. Surprisingly, VWLM
243 was more closely related to climate, particularly to MAP, than any other anatomical
244 trait. This suggests that these two metrics, VWLR and $(t/b)_h^2$ could be describing a
245 slightly different ecological axis of variation, with the latter especially related to
246 investment in support tissue in addition to water availability. Although VWLM could
247 only be used to detect broad MAP differences among fossil assemblages, its real value
248 lies in its use in combination with additional functional traits estimated with other
249 anatomical variables (e.g., hydraulic conductivity, wood density) to better describe
250 fossil forest functional strategies.

251

252 **Acknowledgments**

253 This research was funded by Secretaría de Investigación y Posgrado – Instituto

254 Politécnico Nacional (20220097) grant to E.E.R.

255

256 **Supplementary data**

257 Supplemental material for this article can be accessed here: <URL added by journal>

258 **Table S1.** Localities and climate variables.

259 **Table S2.** Results of the Shapiro-Wilk test for VWLR in extant localities.

260 **Table S3.** Games-Howell test for the entire database results.

261 **Table S4.** Games-Howell test results a subset including only semi-deciduous and wet

262 tropical communities.

263

264 **Literature cited**

265 Baas P. 1986. Ecological patterns in xylem anatomy. In: Givnish, T, J. (Ed.), On the
266 economy of plant form and function. Cambridge University Press, Cambridge, pp
267 327–349.

268 Brodribb TJ, Feild TS. 2000. Stem hydraulic supply is linked to leaf photosynthetic
269 capacity: evidence from new Caledonian and Tasmanian rainforest. *Plant Cell and*
270 *Environment* **23**: 1381–1388.

271 DOI: <https://doi.org/10.1046/j.1365-3040.2000.00647.x>

272 Carlquist S. 1988. Comparative wood anatomy. Berlin: Springer-Verlag. 436 pp. ISBN:
273 978-3-662-21714-6

274 DOI : <https://doi.org/10.1007/978-3-662-21714-6>

275 Castañeda-Posadas C. 2007. Modelo paleoclimático basado en los caracteres

- 276 anatómicos de la madera de las rocas miocénicas de las regiones de Panotla,
277 Tlaxcala y Chajul, Chiapas. Master Thesis, Instituto de Geología, Universidad
278 Nacional Autónoma de México, 178 pp. (In Spanish).
- 279 Cramer MD, Hoffmann V, Verboom GA. 2008. Nutrient availability moderates
280 transpiration in *Ehrharta calycina*. *New Phytologist* **179**: 1048-1057.
281 DOI: [10.1111/j.1469-8137.2008.02510.x](https://doi.org/10.1111/j.1469-8137.2008.02510.x)
- 282 Fu X, Meinzer FC. 2019. Metrics and proxies for stringency of regulation of plant water
283 status (iso/anisohdry): a global data set reveals coordination and trade-offs
284 among water transport traits. *Tree Physiology* **39**: 122–134.
285 DOI: <https://doi.org/10.1093/treephys/tpy087>
- 286 Hacke UG, Sperry JS. 2001. Functional and ecological xylem anatomy.
287 *Perspectives in Plant Ecology, Evolution and Systematics* **4**: 97–115.
288 DOI: <https://doi.org/10.1078/1433-8319-00017>
- 289 Hacke UG, Sperry JS, Pockman WT, Davis SD, Mcculloh KA. 2001. Trends in wood
290 density and structure are linked to prevention of xylem implosion by negative
291 pressure. *Oecologia* **126**: 457–461.
292 DOI: <https://doi.org/10.1007/s004420100628>
- 293 Jacobsen AL, Ewers FW, Pratt RB, Paddock WA, Davis SD. 2005. Do xylem fibers
294 affect vessel cavitation resistance?. *Plant Physiology* **139**: 546–556.
295 DOI: <https://doi.org/10.1104/pp.104.058404>
- 296 Kolb KJ, Sperry JS. 1999. Differences in drought adaptation between subspecies of
297 sagebrush (*Artemisia tridentata*). *Ecology* **80**: 2373–2384.
298 DOI: <https://doi.org/10.2307/176917>
- 299 Lambers H, Chapin FS, Pons TL. 1998. Plant physiological ecology. New York:
300 Springer-Verlag. 540 pp. ISBN: 978-1-4757-2855-2

- 301 DOI: <https://doi.org/10.1007/978-1-4757-2855-2>
- 302 Machado JL, Tyree MT. 1994. Patterns of hydraulic architecture and water relations of
303 two tropical canopy trees with contrasting leaf phonologies: *Ochroma pyramidale*
304 and *Pseudobombax septenatum*. *Tree Physiology* **14**: 219–240.
305 DOI: <https://doi.org/10.1093/treephys/14.3.219>
- 306 Martínez-Cabrera HI, Cevallos-Ferriz SRS. 2008. Palaeoecology of the Miocene El
307 Cien Formation (Mexico) as determined from wood anatomical characters.
308 *Review of Palaeobotany and Palynology* **150**: 154–167.
309 DOI: <https://doi.org/10.1016/j.revpalbo.2008.01.010>
- 310 Martínez-Cabrera HI, Estrada-Ruiz E. 2014. Wood anatomy reveals high theoretical
311 hydraulic conductivity and low resistance to vessel implosion in Cretaceous fossil
312 forest from northern Mexico. *PLoS ONE* **9**:
313 e108866.[doi:10.1371/journal.pone.0108866](https://doi.org/10.1371/journal.pone.0108866)
- 314 Martínez-Cabrera HI, Jones CS, Espino S, Schenk HJ. 2009. Wood anatomy and wood
315 density in shrubs: responses to varying aridity along transcontinental transects.
316 *American Journal of Botany* **96**: 1388–1398.
317 DOI: <https://doi.org/10.3732/ajb.0800237>
- 318 Martínez-Cabrera HI, Estrada-Ruiz E, Castañeda-Posadas C, Woodcock D. 2012. Wood
319 specific gravity estimation based on wood anatomical traits: Inference of key
320 ecological characteristics in fossil assemblages. *Review of Palaeobotany and*
321 *Palynology* **187**: 1–10.
322 DOI: <https://doi.org/10.1016/j.revpalbo.2012.08.005>
- 323 Muller-Landau HC. 2004. Interspecific and intersite variation in wood specific gravity
324 of tropical trees. *Biotropica* **36**: 20–32.
325 DOI: <https://doi.org/10.1111/j.1744-7429.2004.tb00292.x>

- 326 Poorter L. 2008. The relationships of wood-, gas-, and water fractions of tree stems to
327 performance and life history variation in tropical trees. *Annals of Botany* **102**:
328 367–375.
329 DOI: <https://doi.org/10.1093/aob/mcn103>
- 330 Pratt RB, Ewers FW, Lawson MC, Jacobsen AL, Brediger M, Davis SD. 2005.
331 Mechanism for tolerating freeze-thaw stress of two evergreen chaparral species:
332 *Rhus ovata* and *Malosma laurina* (Anacardiaceae). *American Journal of Botany*
333 **92**: 1102–1113.
334 DOI: <https://doi.org/10.3732/ajb.92.7.1102>
- 335 Santiago LS, Goldstein G, Meinzer FC, Fisher JB, Machado K, Woodruff D, Jones T.
336 2004. Leaf photosynthetic traits scale with hydraulic conductivity and wood
337 density in Panamanian forest canopy trees. *Oecologia* **140**: 543–550.
338 DOI: <https://doi.org/10.1007/s00442-004-1624-1>
- 339 Sperry JS, Pockman WT. 1993. Limitation of transpiration by hydraulic conductance
340 and xylem cavitation in *Betula occidentalis*. *Plant Cell and Environment* **16**: 279–
341 288.
342 DOI: <https://doi.org/10.1111/j.1365-3040.1993.tb00870.x>
- 343 Tyree MT. 2003. Hydraulic limits on tree performance: transpiration, carbon gain and
344 growth of trees. *Trees* **17**: 95–100.
345 DOI: <https://doi.org/10.1007/s00468-002-0227-x>
- 346 Wheeler EA, Baas P, Rodgers S. 2007. Variations in dicot wood anatomy. A global
347 analysis. *IAWA Journal* **28**: 229–258.
348 DOI: <https://doi.org/10.1163/22941932-90001638>
- 349 Wheeler JK, Sperry JS, Hacke UG, Hoang N. 2005. Inter-vessel pitting and cavitation
350 in woody Rosaceae and other vesselled plants: a basis for a safety versus

351 efficiency trade-off in xylem transport. *Plant, Cell and Environment* **28**: 800–812.

352 DOI: <https://doi.org/10.1111/j.1365-3040.2005.01330.x>

353 Zanne AE, Westoby M, Falster DS, Ackerly DD, Loarie SR, et al. 2010. Angiosperm

354 wood structure: Global patterns in vessel anatomy and their relation to wood

355 density and potential conductivity. *American Journal of Botany* **97**: 207–215.

356 DOI: <https://doi.org/10.3732/ajb.0900178>

357 Zimmerman MH. 1983. Xylem structure and ascent of the sap. Berlin: Springer-Verlag.

358 283 pp. ISBN 978-3-642-07768-5

359 DOI: <https://doi.org/10.1007/978-3-662-22627-8>

360

361

362 **Table 1.** Regression coefficients for the relationship between climate variables and

363 vessel wall reinforcement metric.

Trait	MAP	MAT	PET
$(t/b)_h^2$	0.13**	0.05*	0.15*
$(t/b)_{\text{hydraulic}}^2$	0.15**	0.07*	0.22**
$(t/b)_{\text{mean}}^2$	0.25***	0.16**	0.26***
VWLR	0.36***, 0.38***	0.22***, 0.18***	0.32***, 0.03**

*<0.05, **<0.01, <0.001, in regular font database from Fig. 3, n=61; boldface is the combined dataset n=279

364

365

366

367

368

369

370 **Figure legends**

371 **Figure 1.** Relationship between the squared vessel-wall thickness-to-span ratio $(t/b)^2_h$
372 and A. $(t/b)^2_{\text{hydraulic mean}}$. B. $(t/b)^2_{\text{mean}}$. C. VWLR.

373 **Figure 2.** A. Relationship between $(t/b)^2_h$ and $(t/b)^2_{\text{hydraulic mean}}$ predicted P_{50} values. B.
374 Boxplot showing predicted P_{50} values using the original the squared vessel-wall
375 thickness-to-span ratio metric (P_{50h}), the mean hydraulic diameter ($P_{50\text{hydraulic mean}}$), and
376 mean vessel diameter ($P_{50\text{mean}}$). Boxplots show median, interquartile range and largest
377 values within 1.5.times the interquartile range below the 25th and above the 75th
378 percentiles.

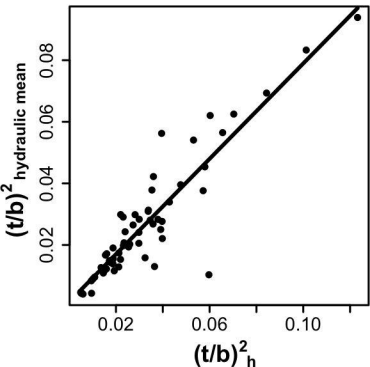
379 **Figure 3.** Climate variables as a function of vessel wall reinforcement metrics. A. MAP.
380 B. MAT. C. PET. The squared vessel-wall thickness-to-span ratio ($(t/b)^2_h$) black
381 squares and dashed line; $(t/b)^2_{\text{mean}}$ red rings and dotted line; $(t/b)^2_{\text{hydraulic mean}}$ light blue
382 triangles and dot-dashed line; VWLR solid orange circles and continuous line.

383 **Figure 4.** VWLR as a function of MAP.

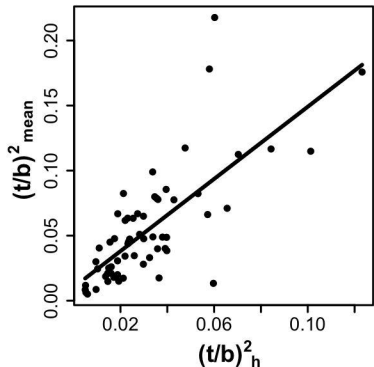
384 **Figure 5.** Comparison of VWLR values across extant and fossil communities. A.
385 Complete dataset. B. Communities from seasonally dry to humid tropical forest and
386 fossil localities. Boxplots show median, interquartile range and largest values within
387 1.5.times the interquartile range below the 25th and above the 75th percentiles.
388 ARG=Argentina, BRA=Brazil, FOS= Fossil localities, MEX=Mexico, SUR= Suriname,
389 USA= United States of America.

390

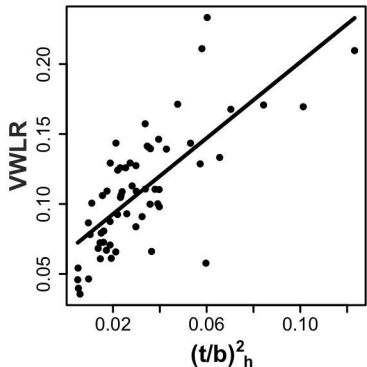
(A)



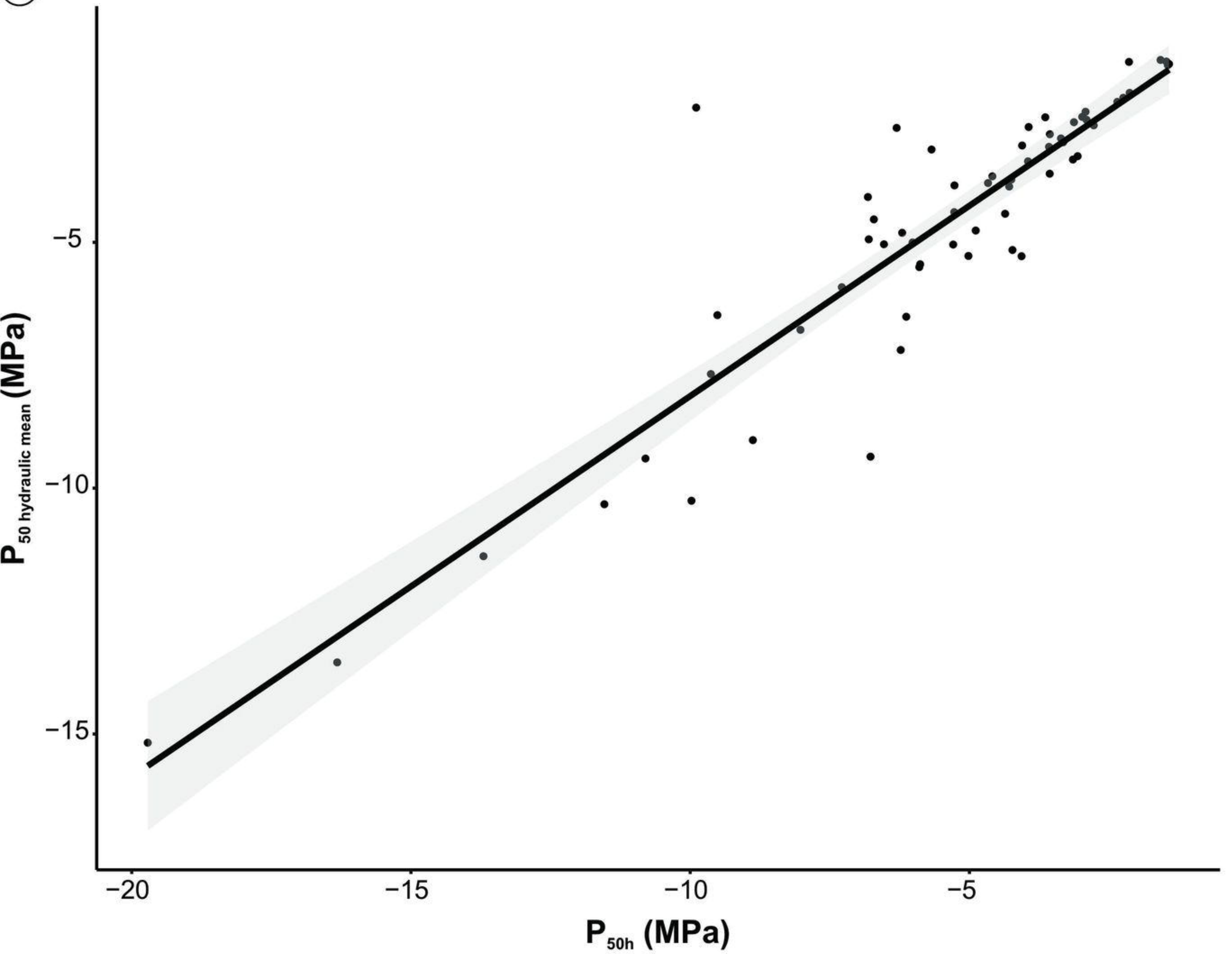
(B)



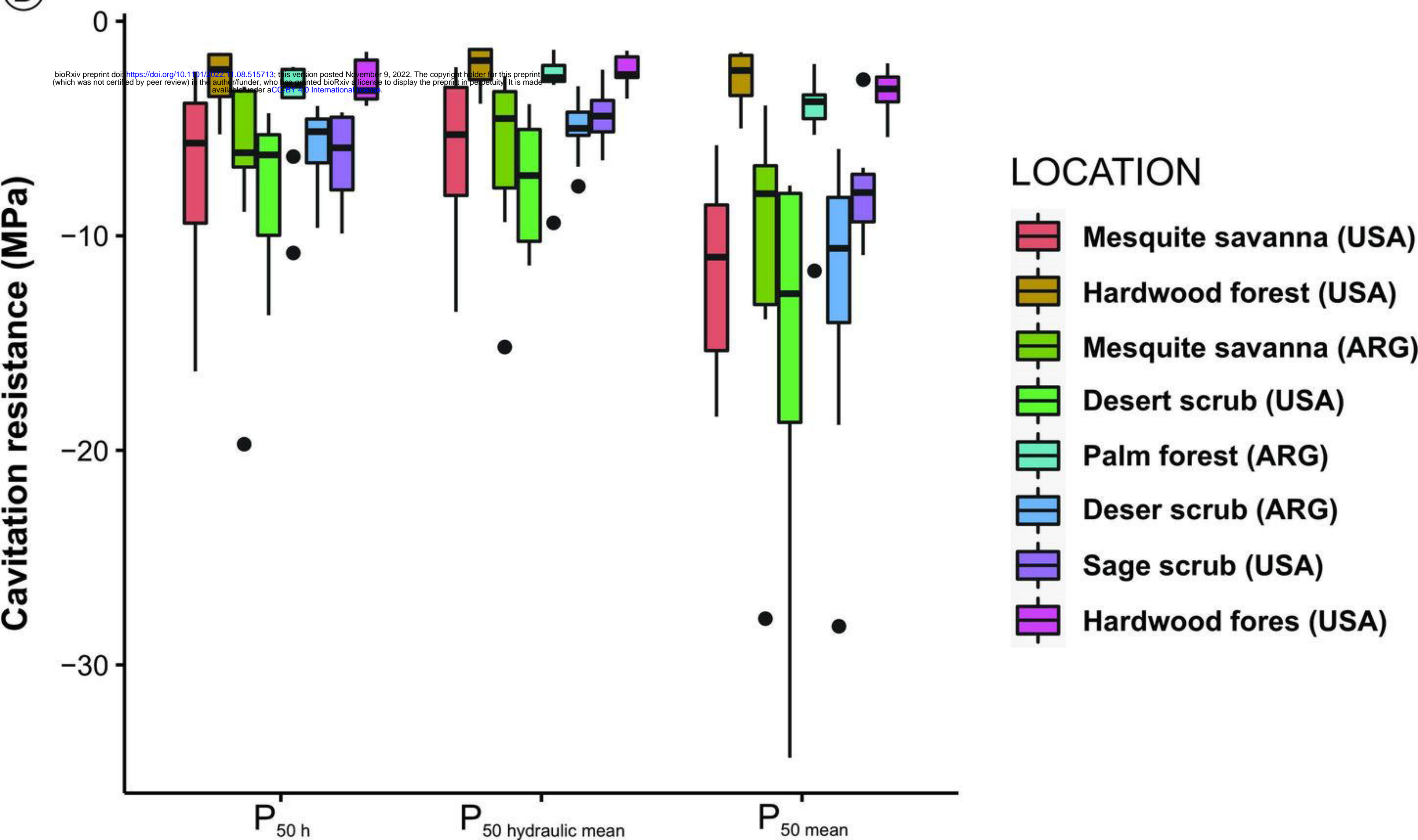
(C)



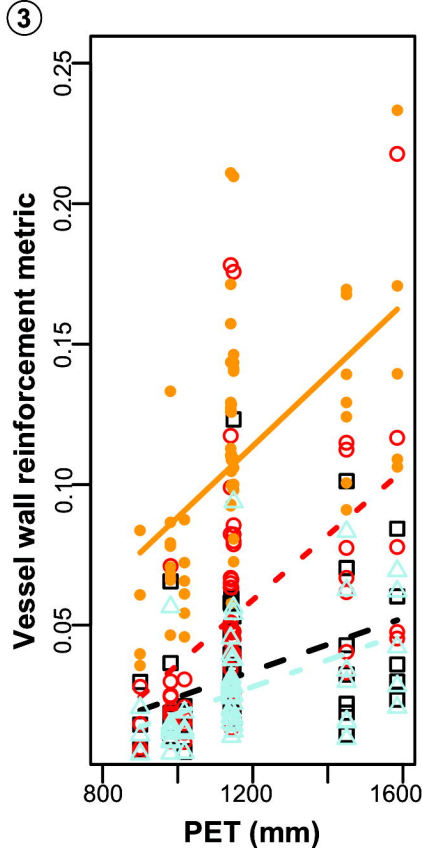
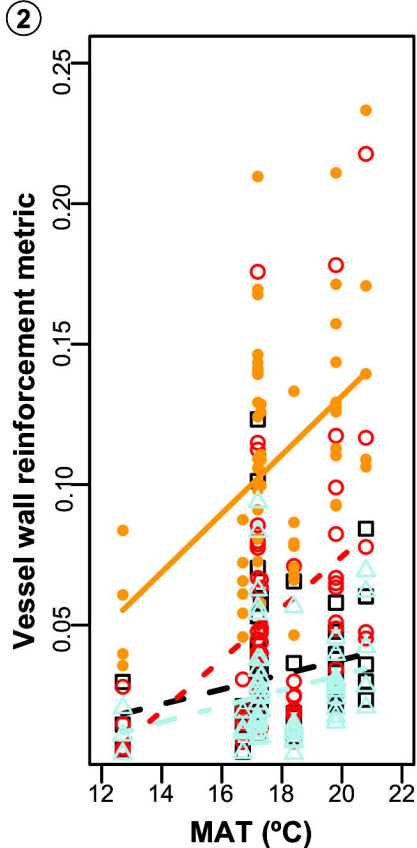
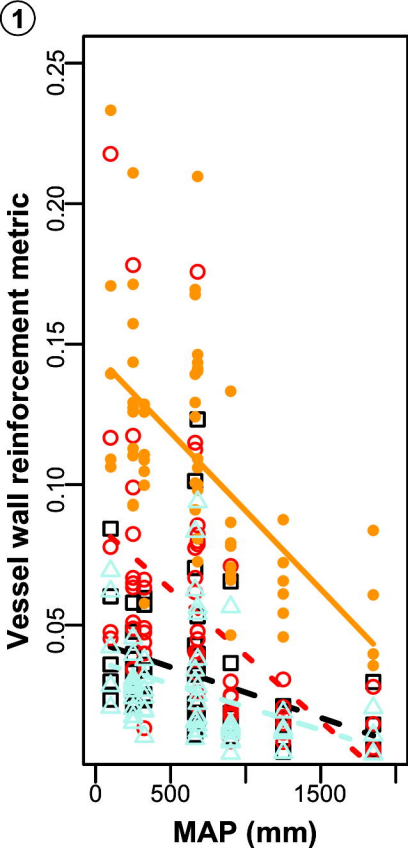
(A)



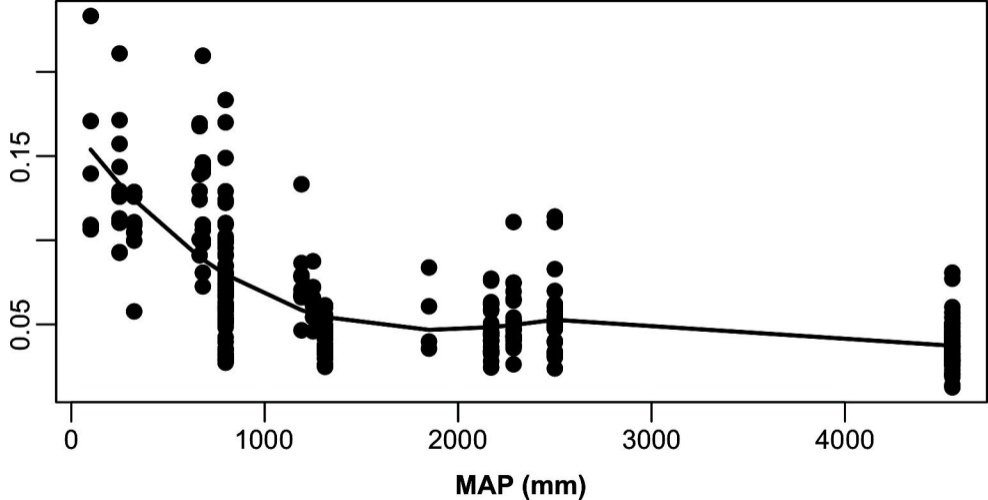
(B)



bioRxiv preprint doi: <https://doi.org/10.1101/2022.11.09.515713>; this version posted November 9, 2022. The copyright holder for this preprint (which was not certified by peer review) is the author/funder, who has granted bioRxiv a license to display the preprint in perpetuity. It is made available under aCC-BY 4.0 International license.

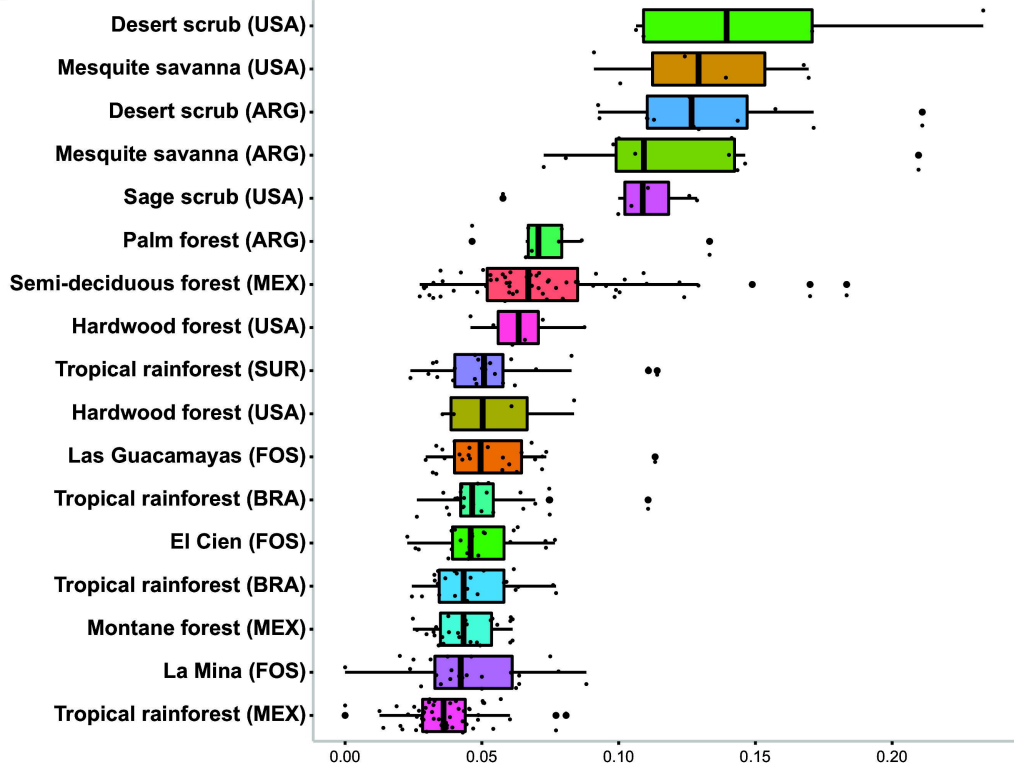


Wall-to-lumen ratio



MAP (mm)

A



B

